ELSEVIER

0144-8617(94)00070-0

Carbohydrate Polymers **26** (1995) 129–140

0144-8617/95/$09.50 + .00

Supermolecular aspects of xanthan–locust bean gum gels based on rheology and electron microscopy

Leif Lundin and Anne-Marie Hermansson

SIK-The Swedish Institute for Food Research, PO Box 5401, S-402 29 Göteborg, Sweden

(Received 7 June 1994; revised version received 26 August 1994; accepted 26 August 1994)

The viscoelastic properties and supermolecular structure of synergistic gels, formed by xanthan and locust bean gum (LBG) of two different mannose:galactose ratios (M:G), have been investigated by small deformation viscoelastic measurements and by low angle rotary-shadowing for transmission electron microscopy.

The rheological properties at 20°C for mixtures subjected to heating and cooling cycles in the temperature range 30–80°C were found to be dependent on the M:G ratio. Mixtures of xanthan and LBG mixed at temperatures $\leq$40°C were found to form true gels with low phase angles. Blends of xanthan and LBG with a low M:G ratio did not show any increase in synergistic effects as the temperature was increased, whilst the mixture of xanthan and LBG with a high M:G ratio showed a strong increase in synergistic effects as the temperature was raised above 60°C. A difference in gelation temperature (T_g) of ~13°C was observed between the mixtures of xanthan and the two LBG fractions. The T_g for xanthan with a high M:G ratio was ~53°C, whilst the T_g for mixtures of xanthan and LBG with a low M:G ratio was ~40°C.

Results obtained using electron microscopy showed that the xanthan–LBG network was formed from xanthan supermolecular strands, and addition of LBG did not influence the xanthan structure. The observed structural features of the gels were independent of heat treatment and LBG fraction. The structural similarities and rheological differences observed between xanthan and the LBG fractions are discussed in comparison with existing interaction models at the molecular level. Based on these results, a speculative network model at the supermolecular level is presented.

INTRODUCTION

Xanthan gum is an exocellular polysaccharide produced by the bacterium *Xanthomonas campestris*. Xanthan is a non-gelling polysaccharide which possesses unique rheological properties such as high viscosity at low concentrations and low shear rates and high pseudoplasticity. The gum consists of β(1-4)D-glucose backbone substituted at C3 on every second residue with a charged trisaccharide side chain containing two D-mannose and one D-glucuronic acid residues. An O-acetyl group is frequently present at the C6 position of the internal mannose residue and pyruvic acid is linked through O-4 and O-6 to the terminal D-mannose residue (Jansson *et al.*, 1975). Recent studies also suggest a partial *O*-acetylation at C6 on the terminal mannose as well as pyruvate (Stankowski *et al.*, 1993).

Xanthan's secondary structure has been investigated by X-ray diffraction and has been shown to consist of a five-fold helical structure (Moorhouse *et al.*, 1977). In solution xanthan undergoes a conformational transition as the physiochemial properties of the solution are altered. An ordered helical conformation is stabilised by high ionic strength and/or low temperatures. The transition midpoint temperature, T_m, is increased as the ionic strength increases, e.g. the helical conformation is stabilised and aggregation is favoured. An increase in T_m has been reported upon addition of a second polymer, such as galactomannans, to the xanthan solution (Dea *et al.*, 1977; Dea & Morris, 1977; Cheetham & Mashimba, 1991). Norton's group has suggested that the equilibrium transition can not be seen as a sharp conformational change occurring at T_m. Instead, the transition can occur in a temperature/ionic strength window within which both states of conformation can occur, although in different proportions (Norton *et al.*,

1984). Xanthan polymer–polymer association is promoted by increasing salt concentration, owing to a reduction in intermolecular repulsion (Smith *et al.*, 1981). Microscopic techniques have been used to visualise the xanthan gum. In order to evaluate the supermolecular structure of xanthan Stokke *et al.* have performed electron microscopy of dilute xanthan glycerol solution which was vacuum-dried and then rotary shadowed (Stokke *et al.*, 1986*a*, 1986*b*, 1987, 1989*a*, 1989*b*). Recently, scanning tunnelling microscopy has been performed on xanthan gum (Gunning *et al.*, 1993; Wilkins *et al.*, 1993).

Locust bean gum (LBG) or carob gum is a galactomannan occurring naturally in seeds of *Ceratonia siliqua*. LBG is a non-gelling neutral polysaccharide which has highly viscous properties and is relatively stable against variations in pH, salinity and temperature. The polysaccharide consists of a $\beta(1\rightarrow4)$D-mannose backbone which is incompletely and irregularly substituted at C6 with α-D-galactose. The mannose to galactose ratio, M:G, is dependent on the source of galactomannan and the method of extraction. Galactose substitution enhances the dissolution properties of the galactomannan. It is thus possible to separate LBG into different M:G fractions according to the minimum temperature at which water solubility can be attained (Gaisford *et al.*, 1986). Dissolved LBG adopts a disordered, fluctuating, random coil conformation. To our knowledge, the unperturbed LBG random coil structure has never been visualised using microscopic techniques.

Xanthan has been found to form synergistic, elastic, thermoreversible gels when mixed with LBG (Dea & Morrison, 1975; Dea *et al.*, 1977; Morris, 1977). All gelation mechanisms presented to explain the synergistic effects are based on intermolecular binding between xanthan and LBG. The interaction is strongly enhanced as the degree of galactose substitution is decreased. The earliest interaction model proposed an association between the xanthan backbone and unsubstituted regions of the galactomannan (Dea & Morrison, 1975). In order to explain the strong synergism between xanthan and galactomannans with a relatively high M:G ratio, the distribution of galactose along the mannan backbone was taken into account. McCleary *et al.* suggested that xanthan interacts with non-substituted areas of galactomannan as well as with regions which are substituted on one side (McCleary, 1979). Tako has proposed a lock and key interaction between the side chains of helical xanthan and the unsubstituted galactomannan backbone (Tako *et al.*, 1984; Tako, 1991, 1993). Cheetham & Mashimba have presented a network model, based on interaction between xanthan and unsubstituted mannan backbone, which explains network formation in three dimensions. They also suggest that interaction may occur with xanthan in the disordered form (Cheetham & Mashimba, 1988).

Based on X-ray diffraction studies, Cairns *et al.* have proposed that the gelation of xanthan–LBG only occurs if the mixture is heated above the helix–random coil transition temperature, T_m, of xanthan and then cooled (Cairns *et al.*, 1986, 1987). The dependence of xanthan–LBG interaction on the xanthan helix–coil transition has been observed by viscoelastic measurements (Zhan *et al.*, 1993; Mannion *et al.*, 1992), gel-permeation chromatography studies, gel melting point measurements and optical rotation studies (Cheetham & Mashimba, 1988, 1991; Cheetham *et al.*, 1986). Lately, convincing results have been presented for xanthan–LBG gelation occurring without heating above T_m (Mannion *et al.*, 1992; Williams *et al.*, 1991). Mixing xanthan–LBG below T_m led to the formation of weak elastic gels. Mannion *et al.* reported that the gels, when mixed cool, were only slightly dependent upon the galactose content of the galactomannan. Heating the mixtures led to strong elastic gels, the rheological properties of which were highly dependent on the degree of galactose substitution. The model proposed is that gelation can occur by two different mechanisms depending on the preparation method. Mannion *et al.* have discussed the possibility that LBG interacts with xanthan in the ordered form, if the mixture is prepared below T_m, while mixtures which have been heated above T_m form network strands consisting of denatured segments of xanthan binding to LBG (Mannion *et al.*, 1992).

The aim of this study is to investigate the xanthan–LBG network structure at the supermolecular level. The temperature dependence of the synergistic interaction between xanthan and LBG with different degrees of galactose substitution has been studied by transmission electron microscopy and small deformation viscoelastic measurements. The results are discussed with reference to possible models of interaction and a speculative network model at the supermolecular level is presented.

EXPERIMENTAL

Materials

Xanthan (Satiaxarie CX 91, lot no. 115) was purchased from Sanofi Bio-Industries (Paris, France). Locust bean gum (G0753, lot no 40H0160) was purchased from Sigma Chemicals (St Louis, MO, USA).

The pure sodium form of xanthan was prepared by ion-exchange of 0·5% (w/w) xanthan solution at room temperature with a commercial resin (AG 50W-X8, Bio-Rad) and freeze dried, according to a procedure described by Morris & Chilvers (1983). The cation concentration was determined by atomic absorption spectroscopy to 2·8% sodium ions, < 0·01% potassium ions and < 0·15% calcium ions per dry weight xanthan.

LBG was separated into temperature fractions, depending upon the solubility of LBG at different

temperatures, according to the procedure described by Mannion *et al.* (1992). The result was four fractions of LBG with the following solubilities: less than 35°C (LBG35), 35–50°C (LBG50), 50–65°C (LBG65) and 65–80°C (LBG80). 20 g LBG was dispersed and boiled in 80% ethanol for 15 min, cooled in an ice–water bath to room temperature and the ethanol decanted. The residue was washed in two 100 ml aliquots of 50% ethanol. The washed LBG was suspended in 2·0 dm^3 distilled water for 1 h at 35°C in a water bath. The suspension was centrifuged for 1 h at 27000 **g**, in order to remove the LBG insoluble at this temperature. The supernatant was collected and freeze dried. The pellet was resuspended for 1 h in 2·0 dm^3 distilled water at 50°C in a water bath. The suspension was treated as above and the procedure was repeated at 65°C and 80°C. The fractions used in this study were LBG35 and LBG80. The respective ratios of mannose to galactose (M:G) were determined, by gas chromatography of their alditol acetate derivatives, to be 3 LBG35 and 5 LBG80 (Bittner *et al.*, 1980).

Sample preparation

The two polysaccharides were dispersed separately in distilled water with 5 mg/dm^3 (8×10^{-5} M) sodium azide added, and stirred continuously until dissolved, in an 80°C water bath. The xanthan and LBG temperature fractions were mixed in equal proportions in order to give a total polymer concentration of 0·5% (w/w), unless otherwise stated. The solutions were allowed to cool to room temperature and mixed for 30 s at a high shearing rate. All samples were mixed at room temperature. In order to evacuate trapped air-bubbles the mixture was centrifuged for 5 min, at 500 **g**. Samples for rheological measurements were transferred immediately after mixing and centrifuging to the Bohlin VOR Rheometer. Samples for electron microscopy were diluted with distilled water with 5 mg/dm^3 sodium azide, at the range of 0·025–0·2% (w/w).

Electron microscopy

In order to visualise and evaluate the temperature dependence of xanthan–LBG, network structure samples of xanthan, LBG35, LBG80 and xanthan–LBG35 and xanthan–LBG80 were prepared for electron microscopy. The mixtures were either mixed at room temperature or mixed at room temperature, heated to 80°C and cooled to room temperature. All pure samples were diluted from 0·5% (w/w) stock solutions to a total polymer concentration of 0·025% (w/w) for xanthan and 0·10% (w/w) of LBG. Mixtures of xanthan–LBG35 were diluted at room temperature to a total polymer concentration of 0·05% (w/w). The heated xanthan–LBG35 was allowed to cool to room temperature before dilution. Xanthan–LBG80 prepared at room temperature was mixed at a concentration of 0·2% (w/w). The heated xanthan–LBG80 was mixed with a total polymer concentration of 0·1% (w/w) at room temperature, heated to 80°C and applied to the mica surface at 80°C. Samples were prepared for electron microscopy using the mica sandwich technique (Hermansson, 1989). This method is suitable for visualisation of supermolecular structures of polymers and polymer mixtures. The samples were applied on a newly cleft mica surface with a minimum of shear, and the other piece of mica plate was gently replaced on top. The mica plate was made as thin as possible in order to get the best heat transport through the plate. The mica 'sandwich' was rapidly plunged into liquid propane or nitrogen and the pieces of mica were separated under the liquid surface. The sample was rapidly transported to a precooled Balzar BAF 400 D (Balzar Union Aktiengesellschaft, Fürstentum, Liechtenstein) freeze etching system, freeze dried at −90°C for 2 h at a pressure of $<10^{-4}$ Pa, and rotary shadowed with 0·8 nm Pt/C at 6° and 20 nm C at 80°. Replicas were collected on 400 mesh Cu grids and examined in a JEOL 100CX-II, at an accelerating voltage of 80 kV.

In order to evaluate the most suitable preparation method, several alternative techniques were evaluated for the pure polysaccharides. The polymer solutions were transferred to the mica surface using spraying or, when the mica sandwich technique was used by pipette or a loop of Pt-wire. The mica sandwich samples were freeze dried at −90°C for 2 h at room temperature for 1 h with no temperature control other than that the starting temperature was approximated to −100°C. The spraying technique was used for samples containing 70% glycerol and samples with no additives. The sprayed samples were vacuum dried at room temperature for 1 h. It was observed that the polymers seemed orientated and possibly aggregated, when the spraying technique was used for samples of LBG. This behaviour may be attributed to the fact that solution flow and surface tension may deform the polymer during the drying process and polymer conformation changes and/or aggregation may be induced due to salt and concentration effects during drying (Hermansson, 1989; Stokke *et al.*, 1989*b*). No major differences were observed for the xanthan samples. It seems that it is only possible to use spraying techniques if the polymer structure is stable enough to resist structural influences induced by drying and by the method used to apply the polymer to the mica surface.

The best results were obtained with the mica sandwich technique in combination with sublimation at −90°C for 2 h. When this technique was applied to LBG samples, the random coil structure was not recognisable. Certain areas of the replica, featuring non-satisfactorily frozen and dried LBG, showed orientated polymers. Although the mica sandwich technique sublimation is time consuming, all micrographs presented in this paper are produced by this technique. Several

preparations were made from every sample and representative micrographs are presented.

Rheological measurements

Rheological measurements were performed in a Bohlin VOR Rheometer (Bohlin Rheology, Lund, Sweden). The measuring geometry was a couette type cup and bob measuring system (DIN 53019). The bob was suspended in an interchangeable torsion bar with a torque at maximum deflection of 5×10^{-4} Nm for dynamic measurements. A layer of paraffin oil was applied on the surface of the sample in order to prevent evaporation. The frequency was 1 Hz when the temperature was varied. As biopolymer gels are strain-sensitive, the strain was kept low, 10^{-3}, so as not to disturb the gel. This was well within the linear region. The viscoelastic properties were recorded during heating and cooling cycles, where the temperature was varied linearly at a rate of 1·5 C/min. Every temperature cycle started at 20 C, the temperature was increased to 30 C and cooled to 20 C. This procedure was repeated with a 10 C increase of the maximum temperature per cycle until 80 C was reached. A holding time of 15 min was applied at 20 C and at the maximum temperature. This repetitive temperature cycling was performed in order to generate an increased degree of xanthan disordering. Viscoelastic measurements were performed on xanthan–LBG35 and xanthan LBG80. One set of measurements was performed at a constant total polymer concentration, 0·5% (w/w), varying the mixing ratio. Another set was performed at a constant xanthan concentration, 0·25% (w/w), varying the LBG concentration from 0·1 to 0·5% (w/w).

RESULTS

Electron microscopy

Xanthan and LBG have been studied extensively using different techniques such as optical rotation, X-ray diffraction, viscoelastic measurements, etc. (Dea & Clark, 1986; Cairns *et al.*, 1986; Doublier& Llamas, 1991; Tako, 1993; Doublier *et al.*, 1992). The mica sandwich technique has been applied to xanthan, LBG and xanthan–LBG mixtures in order to study the supermolecular structure. This method generates the possibility of visualising a monolayer of polymers adsorbed to a mica surface at high resolution. To our knowledge, no micrographs of xanthan LBG networks have ever been presented.

Xanthan

Xanthan has previously been studied in the electron microscope at relatively low concentrations in the range of 0·0003–0·005% (w/v), in order to observe individual superstrands (Stokke *et al.*, 1986*a*, 1986*b*, 1987, 1989*a*, 1989*b*). The concentration of xanthan used in this study was 0·025% (w/w). At the concentration used, the polymer density varies along the mica surfaces. In certain areas of the mica surface, where polymer concentration is high enough, it is possible to study the entanglement structure of xanthan. These areas are represented in the micrograph in Fig. 1, which shows randomly entangled superstrands of xanthan forming a network on the mica surface. The thickness of the coarse strands varies, which indicates a non-uniform number of xanthan helices per strand.

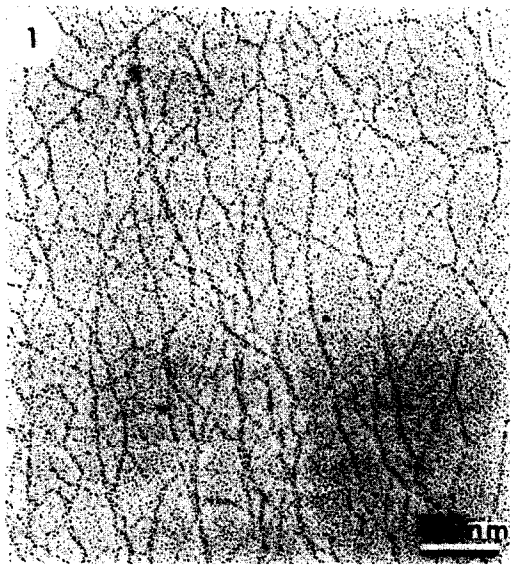

Fig. 1. Micrograph of xanthan showing the supermolecular structure of xanthan.

Locust bean gum

The micrographs of LBG are obtained from a monolayer of polymers adsorbed to the mica surface. Figures 2a and b show the very fine structure of LBG35 and LBG80, respectively. The random coil structure is hardly seen, since it is close to the resolution obtained with the rotary shadowing technique. However, the methods of preparation can induce visible structures. In Fig. 3, shear induced LBG35 structure can be seen as parallel strands going from the lower left-hand to the upper right-hand corner. The structure is probably formed owing to the shearing of LBG polymers when the mica plates were put together. The stress thereby applied orientates the polymers leading to visible structures of LBG.

Xanthan LBG

Figures 4a and b and 5a and b present micrographs of the polysaccharide mixtures. Figure 4a and b shows the network structure of xanthan–LBG35 and xanthan LBG80, respectively, prepared at room temperature. The network is formed by supermolecular xanthan strands. A slight tendency for the supermolecular

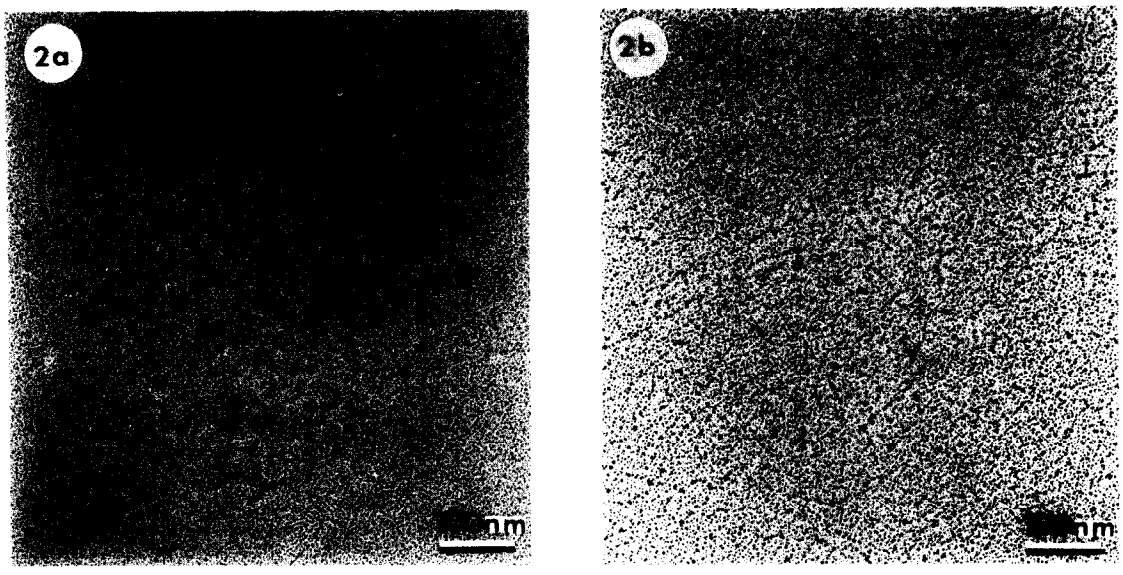

Fig. 2. Micrograph of (a) LBG35 and (b) LBG80 showing the random coil structure.

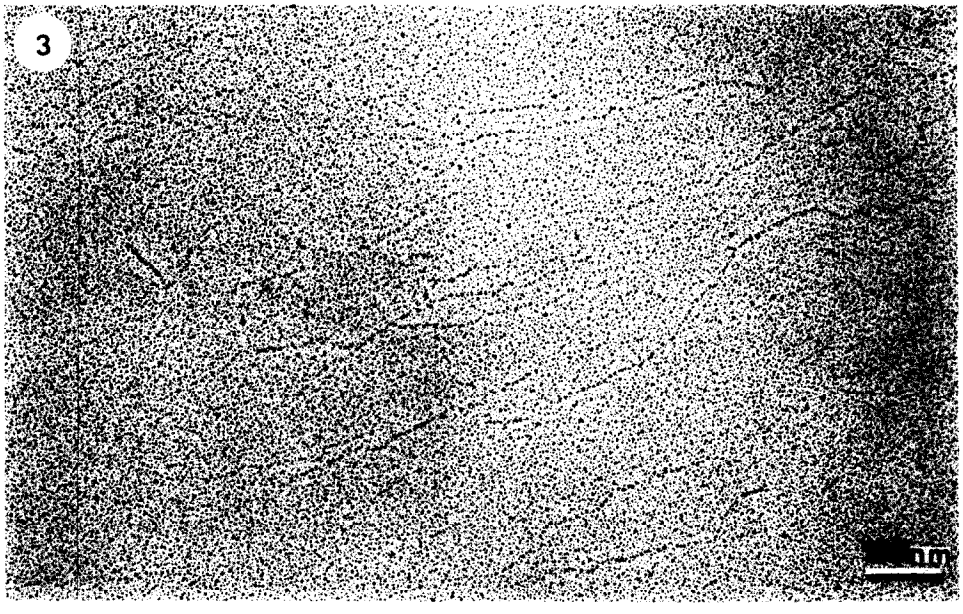

Fig. 3. Micrograph of LBG35 showing random coil and shear induced structures.

strands to form bundles is observed. It should be mentioned that bundles of supermolecular xanthan have also been seen in micrographs of pure xanthan, but these are not as predominant as in the xanthan–LBG mixtures. Figures 5a and b show xanthan–LBG mixtures subject to heating. These mixtures have been heated to 80°C and then cooled to room temperature. The micrographs show the structure of xanthan–LBG at room temperature. The networks formed do not differ structurally from the networks formed at room temperature without heating. The coarse network is formed of xanthan supermolecular strands, and it is not possible to detect any interaction between xanthan helices and LBG. The slight tendency for bundling of supermolecular xanthan strands is also observed.

It is very interesting to note that the supermolecular structure of xanthan does not seem to be perturbed by addition of LBG, and the structure is independent of LBG fraction and heating temperature. It is not possible to observe any structural differences between xanthan and LBG networks and the supermolecular strands of pure xanthan, other than a slightly higher tendency for the mixtures to form bundles. It should be noted that LBG random coils cannot be seen in the micrographs and that no interaction between xanthan and LBG is detectable at the molecular level. LBG is of completely

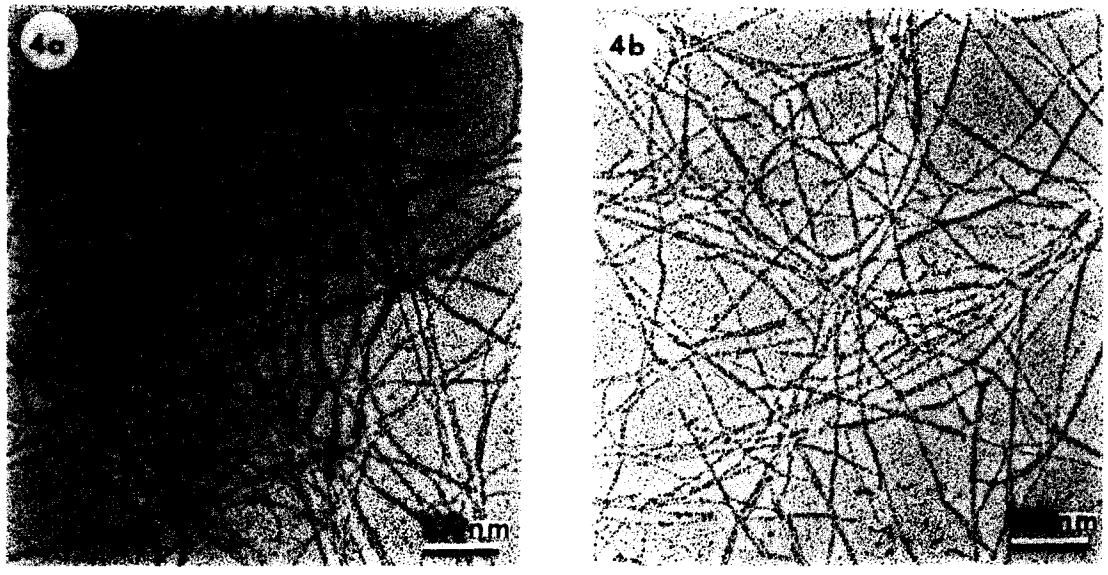

Fig. 4. Micrograph showing the network structure of (a) xanthan–LBG35 and (b) xanthan–LBG80, mixed at room temperature.

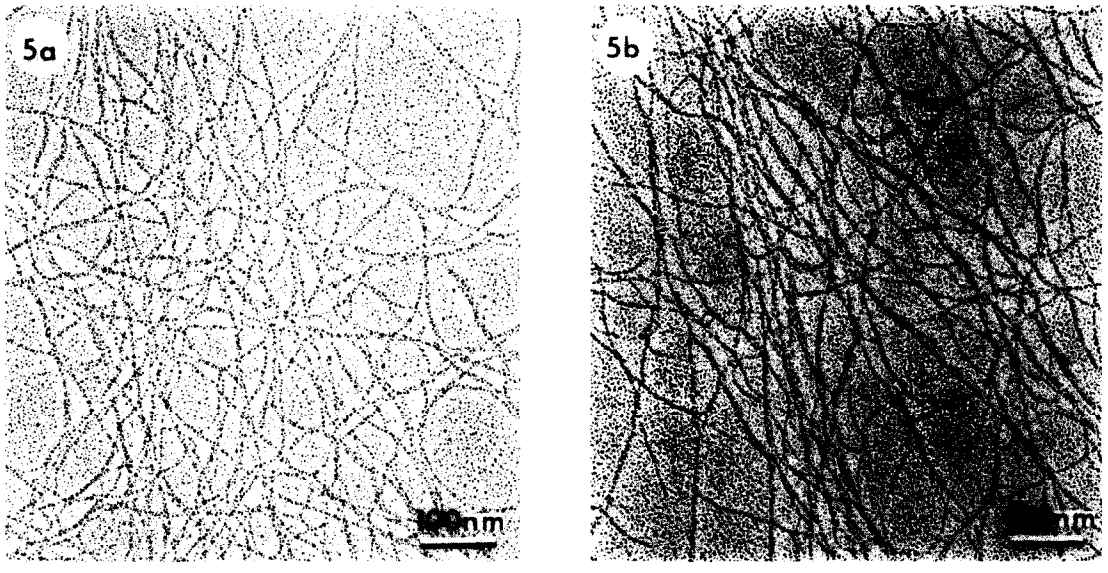

Fig. 5. Micrograph showing the network structure of (a) xanthan LBG35 and (b) xanthan–LBG80, heated to 80°C and then cooled to room temperature.

different dimensions to the stiff supermolecular xanthan strands. The micrographs do not show any evidence of microscopic aggregation of the single polymers leading to phase separation.

Rheology

Viscoelastic properties of xanthan–LBG mixtures

Xanthan–LBG shows extraordinary rheological features when mixed. Figure 6 shows the storage modulus, G', at 20°C after the last temperature cycle presented at a total polymer concentration of 0·5% (w/w), and different mixing ratios of xanthan:LBG35 and xanthan:LBG80. Optimum synergism is observed for xanthan–LBG35 in the range of 4:6 to 6:4 and for the xanthan–LBG80 system between the ratio 4:6 and 1:1. The optimal mixing ratio is in the range of ratios presented for blends containing unfractionated LBG (Tonon & Launay, 1988; Cuvelier & Launay, 1988; Tako, 1991). The magnitude of the synergism was strongly dependent on the M:G ratio of the LBG. The storage moduli for a 1:1 mixture were found to be 140 Pa for the LBG80 system and 33 Pa for the xanthan–LBG35 mixture. These results are in agreement with those of McCleary (1979), McCleary *et al.*, (1981, 1985) and Dea & Clark (1986), showing that the interaction

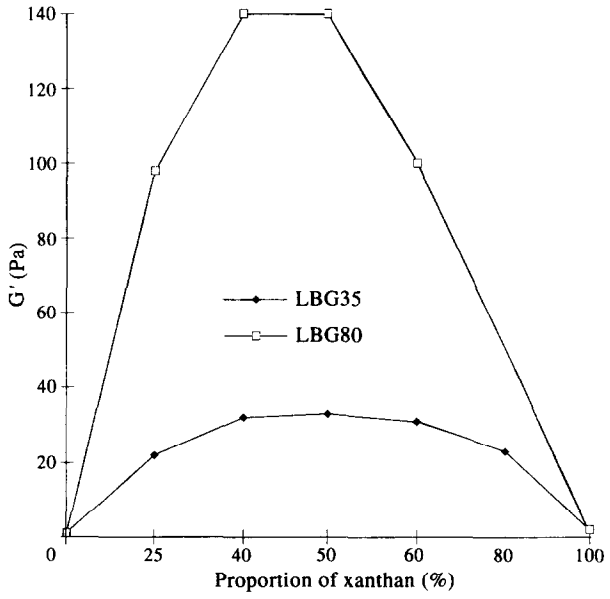

Fig. 6. Storage modulus (G') at 20°C as a function of xanthan LBG35 and LBG80 mixing ratio, respectively. The mixtures have been subjected to heating to 80°C.

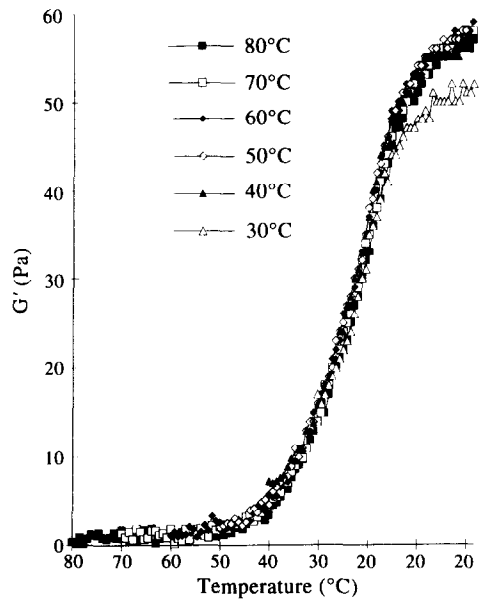

Fig. 7. The storage modulus (G') as a function of temperature for a mixture of 0·25% (w/w) xanthan and 0·5% (w/w) LBG35. The mixture has been subjected to temperature cycling.

between xanthan and galactomannan is dependent on M:G ratio and substitution distribution of the galactomannan. The same value of G' was observed for a blend subjected to the full temperature cycles, as compared with a mixture only exposed to one temperature cycle to 80°C and then cooled, i.e. the repetitive temperature cycling to which the polysaccharide mixtures are subjected does not influence the ultimate rheological properties of the gel if the two preparations are compared. It is also noteworthy that all mixtures studied formed gels after heating to 80°C. These elastic networks with a constant total polymer concentration showed phase angles $\leq 8°$ for the xanthan–LBG35 system and $\leq 4°$ for the xanthan–LBG80 system.

Temperature dependence of the storage moduli

Systems containing a constant xanthan concentration of 0·25% (w/w) and varying amounts of LBG, 0·1–0·5% (w/w), i.e. a total polymer concentration of 0·35–0·75% (w/w), have been subjected to repetitive temperature cycling between 20 and 80°C. Mixtures of xanthan–LBG35 and xanthan–LBG80 have been investigated. Figures 7 and 8 show G' as a function of temperature of xanthan–LBG35 and xanthan–LBG80 systems, respectively, with a LBG concentration of 0·5% (w/w), during the temperature cycles. The other mixtures with lower LBG concentrations show the same behaviour, although not as explicitly. The features to be observed are most clearly shown for this concentration. As shown in Fig. 7, the gel strength of the xanthan–LBG35 gel is independent of temperature history, although a slight increase in G' is observed after the 40°C cycle. This is probably attributable to an increased mixing of polymers and dissociation of xanthan helices. The phase angle for the mixture is constant about 8°, and is independent of temperature heating.

As shown in Fig. 8, the rheological features of the xanthan–LBG80 mixture are strongly influenced by temperature cycling. G' is sharply increased as the cycling temperature is increased above 40°C. As the cycling temperature is raised from 30 to 80°C the phase angle decreases from about 10° to less than 1°. Thus the phase angle is low even for the blends not subjected to temperatures above 40°C. Temperature cycling above 60°C did not have any significant effect on G' for the xanthan–LBG80 mixture. The interaction between xanthan and LBG80 is strongly dependent on temperature before cooling.

Figures 9 and 10 show G' at 20°C for mixtures of xanthan and LBG35 or LBG80 at concentrations between 0·1 and 0·5% (w/w), which have been subjected to temperature cycling. Figure 9 reveals that for a certain LBG35 concentration the xanthan–LBG35 blends do not show any increased synergism as the temperature is elevated, although an increase in G' is noted as the LBG35 concentration is increased. This may be due to an increased total polymer concentration from 0·35 to 0·75% (w/w) or to an increased number of unsubstituted LBG35 interaction sites available for synergism with xanthan. The phase angle for the xanthan–LBG35 system decreases from about 8° to 1° as the LBG35 concentration is lowered from 0·5% (w/w) to 0·1% (w/w). This is probably due to a decrease in concentration of flexible non-interactive mannan backbone as the

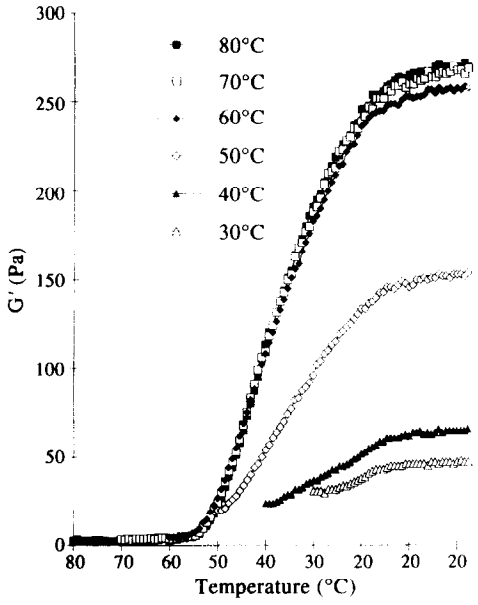

Fig. 8. The storage modulus (G') as a function of temperature for a mixture of 0·25% (w/w) xanthan and 0·5% (w/w) LBG80. The mixture has been subjected to temperature cycling.

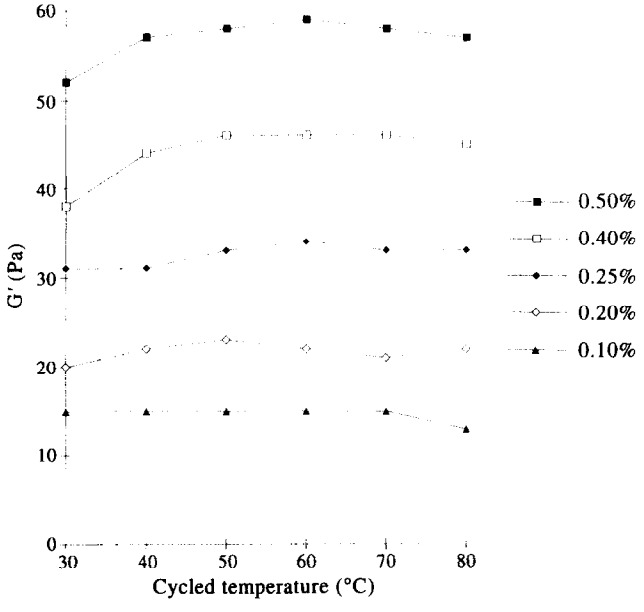

Fig. 9. Storage modulus (G') at 20°C as a function of maximum cycling temperature for mixtures of 0·25% (w/w) xanthan and 0·1–0·5% (w/w) LBG35.

LBG concentration is lowered, leading to a more elastic behaviour.

Figure 10 shows that xanthan–LBG80 exhibits a strong temperature dependence which becomes more pronounced as the LBG80 concentration is elevated. Strong synergistic effects are observed. G' at 20°C increases from 34 to 270 Pa when the LBG80 concentration is increased from 0·1% (w/w) to 0·5% (w/w). This increase in gel strength cannot only be referred to

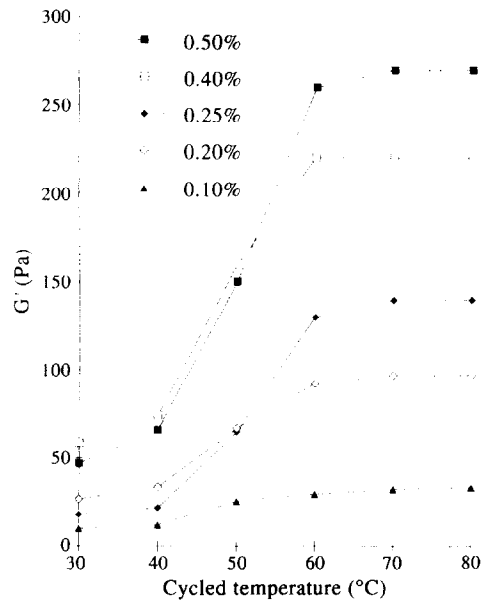

Fig. 10. Storage modulus (G') at 20°C as a function of maximum cycling temperature for mixtures of 0·25% (w/w) xanthan and 0·1–0·5% (w/w) LBG80.

as an increase in total polymer concentration. It seems as if when the temperature is elevated between 40 and 60°C the largest increase in G' is observed, while a further increase in temperature does not have any real rheological significance. As the temperature is increased the phase angles for the xanthan systems with different concentrations of LBG80 are decreased, and after the 80°C cycle the phase angles are $\leq 1°$ for any of the systems. This is indicative of highly elastic gels.

Figures 9 and 10 also show that mixtures not subjected to temperatures above 40°C form relatively strong structures. The xanthan–LBG80 and xanthan–LBG35 mixtures subjected to the 30°C cycle have values of G' in the range of 10–60 Pa. The strength is probably highly dependent on the mixing procedure and degree of xanthan aggregation, which leads to a restriction in possible interactions between xanthan and LBG. For the xanthan–LBG80 mixtures, subjected to temperatures below 50°C, a higher G' is actually observed for mixtures with LBG concentrations (0·7% (w/w) as compared with 0·5% (w/w) and 0·2% (w/w) as compared with 0·25% (w/w)). When these mixtures are subjected to temperatures above 50°C, G' for the system with the highest LBG concentration shows the highest G'. This behaviour could be referred to as incomplete mixing and thereby restrictions in possible interactions for xanthan–LBG.

T_g *dependence on LBG fraction*

Figures 11 and 12 depict G' and G'' for the last cooling cycle, 80°C to 20°C of xanthan–LBG35 and xanthan–LBG80, respectively. In this case T_g is taken as the cross-over when $G' = G''$. It is seen that T_g is in the

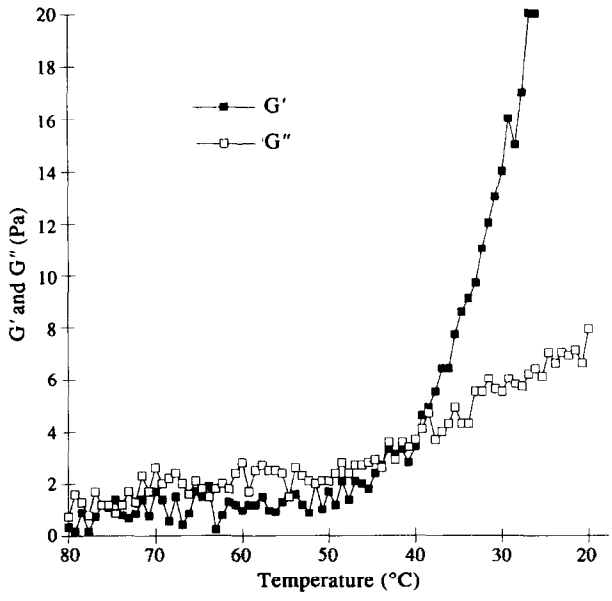

Fig. 11. The temperature dependence of storage (G') and loss (G'') moduli during cooling from 80°C of a mixture of 0·25% (w/w) xanthan and 0·5% (w/w) LBG35.

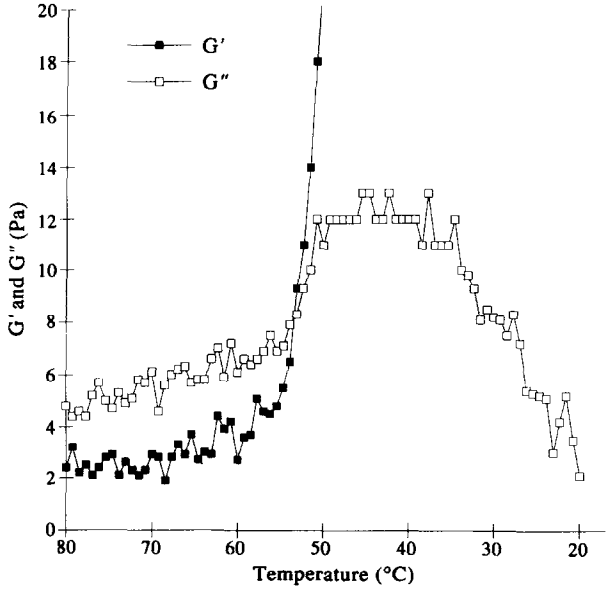

Fig. 12. The temperature dependence of storage (G') and loss (G'') moduli during cooling from 80°C of a mixture of 0·25% (w/w) xanthan and 0·5% (w/w) LBG80.

range of 40°C for xanthan–LBG35 and in the range of 53°C for xanthan–LBG80. It was found for xanthan-LBG35 and xanthan–LBG80 mixtures that T_g only varied a couple of degrees from the values given above, when the LBG concentration was altered in the range 0·1–0·5% (w/w).

The xanthan–LBG35 system (Fig. 11) shows behaviour typical of a gel which is not dependent on a phase transition. Both G' and G'' increase slowly, and there is no pronounced drop in G'' as the temperature is lowered, leading to a gel with a relatively high phase angle. The slow interaction between xanthan and LBG35 seems to take place at temperatures below the xanthan coil–helix transition.

The xanthan–LBG80 mixture (Fig. 12) shows typical features for a fast interaction, with G' increasing steeply and G'' dropping as the temperature is lowered below T_g, leading to a highly elastic gel.

DISCUSSION

The interaction between xanthan and LBG has been well documented (Dea *et al.*, 1977; Morris, 1977; McCleary, 1979 etc.). In agreement with McCleary (1979), our results indicate strong synergistic effects for mixtures of xanthan–LBG, and that these effects are most predominant for xanthan–LBG mixtures containing LBG with a high M:G ratio. It has been reported that the xanthan–LBG interaction is enhanced if the temperature of the mixture is raised above the xanthan transition temperature (Zhan *et al.*, 1993; Mannion *et al.*, 1992; Cheetham & Mashimba, 1988; Cairns *et al.*, 1986). It should be noted that most of these studies have been performed on unfractionated LBG. Our results show that the strongest synergistic effects are obtained for mixtures containing LBG with the highest M:G ratio, i.e. xanthan–LBG80 as compared with blends of xanthan–LBG35 (Fig. 6). This is due to differences in galactose substitution, where a high degree of substitution inhibits the xanthan–LBG interaction (McCleary *et al.*, 1981; Dea & Clark, 1986).

Most models presented for xanthan–LBG mixtures try to explain interactions but do not give a three-dimensional picture of the xanthan–LBG network responsible for the synergistic effects (Morris, 1977; Dea *et al.*, 1977; McCleary, 1979; Tako *et al.*, 1984; Tako, 1993). Cairns *et al.* (1986, 1987) have presented a two-dimensional sandwich model, and Cheetham & Mashimba (1988) have tried to extend their models to three dimensions in order to explain the growth of a network. Our results are presented in order to explain the behaviour of xanthan–LBG mixtures at the supermolecular level.

The micrographs of xanthan–LBG mixtures indicate that the formation of xanthan supermolecular strands is not hindered by the presence of LBG. The xanthan phase transition does not seem to be structurally perturbed by the presence of LBG. Neither is it possible to detect any structural differences between xanthan solutions and mixtures containing LBG35 or LBG80 independently if the mixtures have been heated to 80°C or mixed at room temperature.

Viscoelastic measurements of xanthan–LBG35 and xanthan–LBG80 heated to different temperatures have shown that the storage moduli at 20°C of mixtures containing LBG35 remain relatively unchanged (Fig. 9),

while xanthan–LBG80 blends show significant changes in G' (Fig. 10) as the cycling temperature is raised. The exact value of T_m for our xanthan–LBG solutions is not known. Reported values of T_m for xanthan in water are in the region of 45 °C (Dea *et al.*, 1977; Cheetham & Mashimba, 1991; Williams *et al.*, 1991; Takigami *et al.*, 1993; Zhan *et al.*, 1993). According to Dea *et al.*, addition of LBG has a stabilising effect on xanthan and T_m is increased by ~10 °C (Dea *et al.*, 1977). Therefore T_m is estimated to be ~55 °C.

Heating to temperatures up to 40 °C caused gelation of both xanthan–LBG35 and xanthan–LBG80, indicating interactions between ordered xanthan superstrands and LBG. The relatively low phase angles observed for the system mixed at room temperature suggest an elastic network structure. Because no structural differences have been observed in the micrographs, it is possible that LBG35 and LBG80, as they are blended with xanthan at room temperature, interact at the surface of the xanthan superstrands interconnecting these into a network. The gel strength of these mixtures is probably dependent on the mixing procedure, polymer mixing and degree of xanthan aggregation.

Heating the mixture above 60 °C leads to dissociation of xanthan aggregates and a disordering of the xanthan polymers. In addition, a more complete mixing of the polymers is obtained. On cooling, the xanthan–LBG35 network did not show any increase in G' compared with the gels formed from mixtures not heated above 40 °C. It is possible that the relatively low interactive LBG35 is excluded from the xanthan aggregates as they are formed, and that the LBG35 polymers only associate with short regions of the surface of the xanthan superstrands. The network formed would consist of superstrands of xanthan interconnected by LBG35 bridges.

Mixtures of xanthan–LBG80 heated above 60 °C showed a strong synergistic increase in G' on cooling as compared with the blend subjected to 40 °C (Fig. 8). One explanation can be that the relatively high interactive LBG80 is not excluded from the superstrands as the xanthan helices associate, but is able to interact with single xanthan helices as well as to relatively long regions of the surface of the aggregates of xanthan helices. The network would consist of superstrands of xanthan–LBG80 interconnected by LBG80 bridges.

The increase in G' and G'' (Fig. 11) as the temperature is lowered is slow for xanthan–LBG35 blends, and a considerably viscous part is preserved, indicating restrictions in the interaction. The estimated T_m is about 15°C higher than the observed gelation temperature for xanthan–LBG35, which suggests that the synergistic interaction takes place in the ordered state of xanthan. The rapid increase in G' and terminal decrease in G'' for xanthan–LBG80 (Fig. 12) as the temperature is decreased indicates a rapid reaction. The correlation between T_m and T_g suggests that the synergistic interaction between xanthan and LBG80 occurs as the xanthan helices are formed, and that the interaction between xanthan and LBG is competitive with the formation of aggregates of xanthan helices. In addition, unpublished results show that addition of salt to xanthan–LBG mixtures leads to a decrease in network strength probably due to stabilisation of xanthan helices, promotion of xanthan aggregation and, consequently, restrictions of xanthan–LBG interaction.

The storage modulus G' increased with LBG concentration for both mixtures (Figs 9 and 10). Blends of xanthan–LBG80 showed the most significant effects, especially as the temperature was raised above 60 °C. The xanthan–LBG35 systems showed only moderate increases in G' as the LBG35 concentration was increased. The increase in network strength can be explained as being attributable to an increase in total polymer concentration. This effect is probably minor as compared with the effect attributed to a higher number of possible interaction sites of LBG, i.e. regions of unsubstituted mannan backbone. An increase in LBG80 as compared with an equal increase in LBG35 leads to a relatively higher amount of unsubstituted mannan backbone for the LBG80 solution, which could explain why the effect is more predominant for LBG80.

Morris has proposed that the interaction takes place with xanthan in the ordered form, and that differences in rheological properties between cold mixed and heated blends are due to the destruction of network structure when the polymers are mixed (Morris, 1992). Further support for the model favouring interaction with xanthan in the ordered form is presented by Williams *et al.* They have found that $T_m \geq T_g$ for mixtures of xanthan–LBG in water and 0·04 M NaCl, which indicates that xanthan is in the ordered state as the network is formed (Williams *et al.*, 1991). Lately, Williams *et al.*, on the basis of DSC and ESR spectroscopy studies, have proposed a model for the κ-carrageenan–konjac mannan system, where self-aggregated κ-carrageenan helices are supposed to be covered by surface-adsorbed konjac mannan chains (Williams *et al.*, 1993).

Mannion *et al.* have presented results in agreement with our findings. In order to explain the temperature dependence of G' for the mixtures of xanthan and higher temperature fractions of LBG, Mannion *et al.* have suggested that heating gives more complete molecular mixing, a more homogeneous solution with respect to galactomannan self-association, and that the energy input from heating facilitates interactions which are not possible at room temperature. Mannion *et al.*, draw the conclusion that xanthan–LBG may interact by two distinct mechanisms. One takes place at room temperature with xanthan in the helical form, and the other at elevated temperatures where xanthan in the disordered form interacts with LBG (Mannion *et al.*, 1992).

An alternative explanation would be that, owing to the structural similarities between the network formed by heated and unheated blends of either LBG35 or

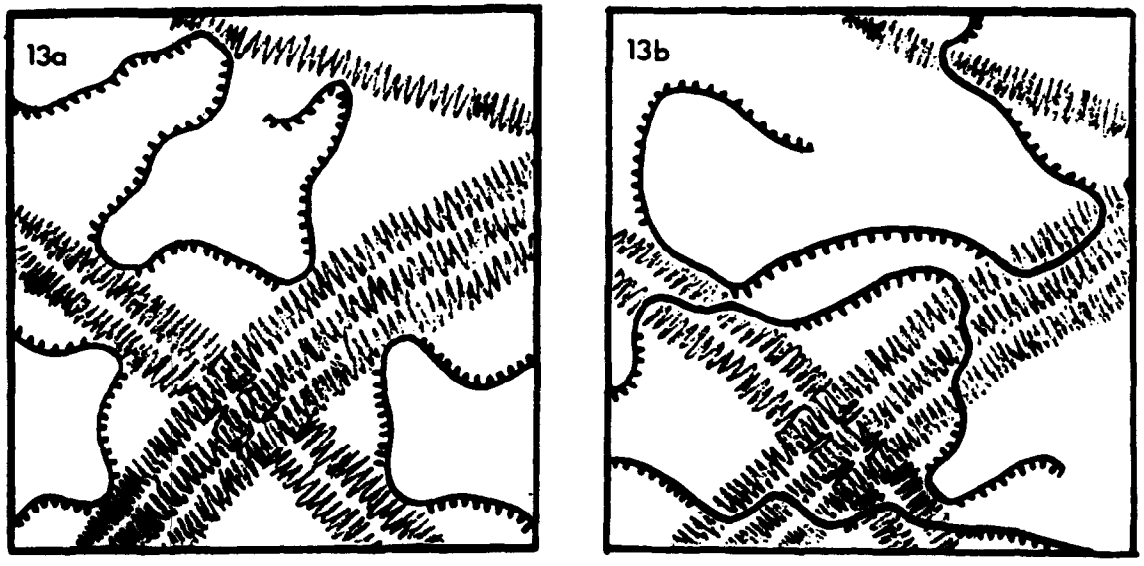

Fig. 13. Schematic model of the xanthan–LBG interaction on the supermolecular level: (a) xanthan–LBG35 network. The network is formed by xanthan superstrands which are interconnected at the surface by relative short regions of LBG35 backbone. (b) Xanthan–LBG80 network. The network is formed by xanthan superstrands which are interconnected and bound together by relatively long areas of LBG80 backbone.

LBG80 and xanthan, there are no differences in interaction mechanisms between the two fractions, and that the interaction occurs with xanthan in the helical form. The synergism observed between xanthan and LBG could be that LBG interconnects supermolecular strands of xanthan through interaction between unsubstituted mannan regions and one or more xanthan strands. A large amount of unsubstituted mannan backbone in combination with helix formation and association of xanthan helices at T_m facilitate the network formation.

In agreement with existing interaction models at the molecular level, with interaction between xanthan and unsubstituted mannan backbone, a network model at the supermolecular level is presented. A schematic representation of the xanthan–LBG network is presented in Fig 13a and b. The speculative model suggests that the much larger xanthan superstrands, as compared with LBG polymers, are connected by bridges of smaller LBG polymers. This means that the supermolecular structure of xanthan is not structurally influenced by the presence of LBG. The binding areas on the LBG polymers are unsubstituted mannan backbone. The difference between the systems containing LBG35 and LBG80 is due to the difference in their degree of galactose substitution. LBG35 polymers are excluded from the xanthan aggregates and can only bind to the surface of the xanthan superstrands (Fig. 13a). LBG80, on the other hand, has a greater tendency to interact, so that LBG80 polymers are not excluded from the aggregates of xanthan helices to the same extent as LBG35. They are, therefore, able to bind to the xanthan helix as well as to the surface of the xanthan superstrands (Fig. 13b). When mixed at room temperature, LBG80 will bind to the surface in the same manner as LBG35. These interactions generate a network with no visible structural differences although the rheological properties of the mixtures are completely different to those of a pure xanthan solution.

The suggested model is supported by the following findings: no structural differences can be observed between heated or unheated mixtures of xanthan and either of the LBG fractions or pure xanthan solutions. There are large rheological differences between mixtures of xanthan and LBG35 or LBG80 after heat treatment. The phase angles for all the gels formed after mixing at room temperature are low. There is a difference in T_g between the mixtures of xanthan–LBG35 and xanthan–LBG80. Heating the xanthan–LBG80 mixture to temperatures $> T_m$ facilitates an increased network strength, whilst no effects are observed for the xanthan–LBG35 mixture.

ACKNOWLEDGEMENTS

Financial support from The Swedish Research Council for Engineering Science (TFR) is gratefully acknowledged. The authors would like to thank Annika Altskär and Elvy Jordansson for expert technical help with microscopy preparation, Ewa Eriksson for guidance with the rheological equipment and Susanne Ekstedt for her excellent network drawings.

REFERENCES

Bittner, A.S., Harris, L.E. & Campbell, W.F. (1980). *J. Agric. Food Chem.*, **28**, 1242 1245.

Cairns, P., Miles, M.J. & Morris, V.J. (1986). *Nature*, **322,** 89–90.

Cairns, P., Miles, M.J., Morris, V.J. & Brownsey, G.J. (1987). *Carbohydr. Res.*, **160,** 411–423.

Cheetham, N.W.H. & Mashimba, E.N.M. (1988). *Carbohydr. Polym.*, **9,** 195–212.

Cheetham, N.W.H. & Mashimba, E.N.M. (1991). *Carbohydr. Polym.*, **14,** 17–27.

Cheetham, N.W.H., McCleary, B.V., Teng, G., Lum, F & Maryanto (1986). *Carbohydr. Polym.*, **6,** 257–268.

Cuvelier, G. & Launay, B. (1988). *Carbohydr. Polym.*, **8,** 271–284.

Dea, I.C.M., Clark, A.H., & McCleary, B.V. (1986). *Carbohydr. Res.*, **147,** 275–294.

Dea, I.C.M. & Morris, E.R. (1977). *Extracellular Microbial Polysaccharides*, eds P.A. Sandford & A. Laskin. ACS Symposium series, Vol. 45, pp. 174–182.

Dea, I.C.M., Morris, E.R., Rees, D.A., Welsh, E.J., Barnes, H.A. & Price, J. (1977). *Carbohydr. Res.*, **57,** 249–272.

Dea, I.C.M. & Morrison, A. (1975). *Adv. Carbohydr. Chem. and Biochem.*, eds R.S. Tipson & D. Horton. Academic Press, New York. Vol. 31, pp. 241–312.

Doublier, J.-L., Castelain, C. & Lefebvre, J. (1992). *Plant Polymeric Carbohydrates*, eds F. Meuser, D.J. Manners & W. Seibel. The RCS Special Publication No. 134, Cambridge, pp. 76–85.

Doublier, J.-L. & Llamas, G. (1991). *Food Polymers, Gels and Colloids*, ed. E. Dickinson. RCS Special Publication No. 82, Cambridge, pp. 349–356.

Gaisford, S.E., Harding, S.E., Mitchell, J.R. & Bradley, T.D. (1986). *Carbohydr. Polym.*, **6,** 423–442.

Gunning, A.P., McMaster, T.J. & Morris, V.J. (1993). *Carbohydr. Polym.*, **21,** 47–51.

Hermansson, A-M. (1989). *Carbohydr. Polym.*, **10,** 163–181.

Jansson, P-E., Kenne, L. & Lindberg, B. (1975). *Carbohydr. Res.*, **45,** 275–282.

McCleary, B.V. (1979). *Carbohydr. Res.*, **71,** 205–230.

McCleary, B.V., Amado, R., Waibel, R. & Neukom, H. (1981). *Carbohydr. Res.*, **92,** 269–285.

McCleary, B.V., Clark, A.H., Dea, I.C.M. & Rees, D.A. (1985). *Carbohydr. Res.*, **92,** 269–260.

Mannion, R.O., Melia, C.D., Launay, B., Cuvelier, G., Hill, S.E., Harding, S.E. & Mitchell, J.R. (1992). *Carbohydr. Polym.*, **19,** 91–97.

Moorhouse, R., Walkinshaw, M.D. & Arnott, S. (1977). *Extracellular Microbial Polysaccharides*, eds P.A. Sandford & A. Laskin. ACS Symposium series, Vol. 45, pp. 90–102.

Morris, E.R. (1977). *Extracellular Microbial Polysaccharides*, eds P.A. Sandford & A. Laskin. ACS Symposium series, Vol. 45, pp. 81-89.

Morris, E.R. (1992). *Food Gels*, ed. P. Harris. Elsevier Applied Science, Barking, pp. 291–359.

Morris, V.J. & Chilvers, G.R. (1983). *Carbohydr. Polym.*, **3,** 129–141.

Norton, I.T., Goodall, D.M., Frangou, I.T., Morris, E.R. & Rees, D.A. (1984). *J. Mol. Biol.*, **175,** 371–394.

Smith, I.H., Symes, K.C., Lawson, C.J. & Morris, E.R. (1981). *Int. J. Biol. Macromol.*, **3,** 129–134.

Stankowski, J.D., Mueller, B.E. & Zeller, S.E. (1993). *Carbohydr. Res.*, **24,** 321–326.

Stokke, B., Elsgaeter, A., Skjåk-Bræk & Smidsrød, O. (1987). *Carbohydr. Res.*, **160,** 13–28.

Stokke, B., Elsgaeter, A. & Smidsrød, O. (1986*a*). *Int. J. Biol. Macromol.*, **8,** 217–225.

Stokke, B., Elsgaeter, A. & Smidsrød, O. (1989*a*). *Am. Chem. Soc.*, **7,** 145–156.

Stokke, B., Smidsrød, O. & Elsgaeter. (1986*b*). *Polym. Mater. Sci. Engng*, **55,** 583–587.

Stokke, B.T., Smidsrød, O. & Elsgaeter, A. (1989*b*). *Biopolymers*, **28,** 617–637.

Takigami, S., Shimida, M., Williams, P.A. & Phillips, G.O. (1993). *Int. J. Biol. Macromol.*, **15,** 367–371.

Tako, M. (1991). *J. Carbohydr. Chem.*, **10,** 619–33.

Tako, M. (1993). *Colloids and Surfaces*, **1,** 125–131.

Tako, M., Asato, A. & Nakamura, S. (1984). *Agric. Biol. Chem.*, **48,** 2995–3000.

Tonon, C. & Launay, B. (1988). *Physical Networks Polymers and Gels*, eds W. Burchard & S.B. Ross-Murphy. Elsevier Applied Science, London, pp. 335–344.

Wilkins, M.J., Davis, M.C., Jackson, D.E., Roberts, C.J. & Tendler, S.J.B. (1993). *J. Microscopy*, **172,** 215–221.

Williams, P.A., Clegg, S.M., Langdon, M.J., Nishinari, K. & Piculell, L. (1993). *Macromolecules*, **26,** 5441–5446.

Williams, P.A., Day, D.H., Langdon, M.J., Phillips, G.O. & Nishinari, K. (1991). *Food Hydrocoll.*, **4,** 489–493.

Zhan, D.F., Ridout, M.J., Brownsey, G.J. & Morris, V.J. (1993). *Carbohydr. Polym.*, **21,** 53–58.